Palaeogeography, Palaeoclimatology, Palaeoecology 659 (2025) 112629

Contents lists available at ScienceDirect

Palaeogeography, Palaeoclimatology, Palaeoecology

journal homepage: www.elsevier.com/locate/palaeo

Simulated isotopic fingerprint of the Atlantic Multidecadal Oscillation over South America and its relation to the Little Ice Age

Jelena Maksic [a,*], Marília Harumi Shimizu [b,e], Gilvan Sampaio [b], Cristiano M. Chiessi [c], Matthias Prange [d], Mathias Vuille [f], Giselle Utida [g], Francisco W. Cruz [c], Murilo Ruv Lemes [a]

[a] Division of Impacts, Adaptation and Vulnerabilities (DIIAV), National Institute for Space Research (INPE), Sao Jose dos Campos, 12227-010, Brazil
[b] General Coordination of Earth Science (CGCT), National Institute for Space Research (INPE), Sao Jose dos Campos, 12227-010, Brazil
[c] School of Arts, Sciences and Humanities, University of Sao Paulo, Sao Paulo 01156-000, Brazil
[d] MARUM—Center for Marine Environmental Sciences and Faculty of Geosciences, University of Bremen, 28359 Bremen, Germany
[e] Graduate Program in Geosciences (Geochemistry), Fluminense Federal University, Niterói, Brazil
[f] Department of Atmospheric and Environmental Sciences, University at Albany, United States
[g] Institute of Geoscience, University of São Paulo, Rua do Lago, 562, Cidade Universitária, São Paulo-SP, 05508-090, Brazil

ARTICLE INFO

Editor Name: Prof. M Elliot

Keywords:
Atlantic Multidecadal Oscillation
Stable oxygen isotope
iCESM1.2
South America
Little Ice Age

ABSTRACT

Linkages have been established between the Atlantic Multidecadal Oscillation (AMO) and surface air temperature variations, low-level jet streams, and precipitation trends in both northeastern Brazil and southeastern South America. Previous studies have discerned distinct wet-season (March–May) precipitation responses in northeastern Brazil, with cold (warm) AMO phases triggering increased (decreased) precipitation. Findings from various records indicate that the AMO's variability extends for thousands of years. A recent reconstruction suggests a significant AMO role in the shift from the Medieval Climate Anomaly (MCA) to the Little Ice Age (LIA) and reveals the LIA as the longest period with a persistent cold anomaly in the North Atlantic over the past ~3 millennia. Stable oxygen isotope records from South America show typical AMO periodicities (~65 years), however, despite increased paleo precipitation data, the AMO's role in South American precipitation during the LIA and MCA remains unclear. In this study, the influence of AMO phases on atmospheric dynamics, precipitation patterns, and stable oxygen isotope composition (δ18O) of precipitation over South America is assessed using the water isotope-enabled version of the Community Earth System Model version 1.2 (iCESM1.2). This research sheds light on the connection between AMO-induced precipitation anomalies and isotopic signals observed in paleoclimate records and emphasizes the significance of isotope-enabled climate models in unraveling the mechanisms behind past variations. The analysis involves comparing δ18O simulations with published reconstructions from South America. By utilizing climate models that incorporate isotopes, we can delve deeper into understanding the impact of the AMO on precipitation patterns and isotopic ratios. Contrary to expectations, the simulated $\delta^{18}O_p$ signal differ from speleothem records over the western Amazon and Andes during the LIA. That is, the simulated significant total precipitation amounts change over the western Amazon and Andes are not reflected in $\delta^{18}O_p$ depletion.

1. Introduction

The Atlantic Multidecadal Oscillation (AMO) is a mode of observed variability in North Atlantic sea surface temperatures (SST) that consists of an alternation between warm and cold SST anomalies (Folland and Kates, 1984; Kushnir, 1994; Schlesinger and Ramankutty, 1994). The alternations between warm and cold anomalies was first identified during the 1980s (Folland and Kates, 1984). Methods for constructing the AMO index (Enfield et al., 2001; Trenberth and Shea, 2006; Guan and Nigam, 2009; Knight, 2009; Ting et al., 2009; Yan et al., 2019) consider different aspects of the basin- or sub-basin scale variability, but all capture large-scale multidecadal SST anomalies. The swings between warm and cold phases are with a period of 60–90 years (Schlesinger and Ramankutty, 1994; Knight et al., 2006). The most recent statistical analysis of instrumental records (Wang et al., 2017; Qin et al., 2020) suggest that AMO is simultaneously modulated by both internal and

* Corresponding author.
E-mail address: maxic.jelena@gmail.com (J. Maksic).

https://doi.org/10.1016/j.palaeo.2024.112629
Received 27 October 2023; Received in revised form 6 October 2024; Accepted 24 November 2024
Available online 2 December 2024

external forcings.

The AMO has a global-scale impact on climate that is well summarized in Zhang et al., 2019. It has an impact on the Atlantic hurricane activity (Zhang and Delworth, 2006), North American and European summer climate (Sutton and Hodson, 2005), African Sahel rainfall (Wang et al., 2012), Asian monsoon (Miao and Jiang, 2021), and summer rainfall over India (Krishnamurthy and Krishnamurthy, 2015).

Studies that analyzed the AMO impacts over South America found linkages with surface air temperature (Kayano and Setzer, 2018), low-level jets (Jones and Carvalho, 2018; Loaiza Cerón et al., 2020), precipitation over northeastern Brazil (Knight et al., 2006; Kayano et al., 2016) and southeastern South America (Seager et al., 2010). For northeastern Brazil, previous studies (Knight et al., 2006; Kayano et al., 2016) found increased (decreased) precipitation induced by cold (warm) AMO during the wet season, i.e., March–May (MAM).

Instrumental records suggest that AMO phases are coupled with the Intertropical Convergence Zone (ITCZ) position (Levine et al., 2018). Modeling studies also recognize changes in the ITCZ position as an important mechanism by which the AMO influences precipitation (Knight et al., 2006; Ting et al., 2011; Levine et al., 2018). Contrary to expectations, results from Maksic et al. (2022) show that AMO-related precipitation anomalies over northeastern South America are mainly related to changes in the Atlantic ITCZ core strength, instead of changes in its position. In the cold (warm) AMO phase, the core ITCZ region strengthens (weakens) from February to July, while from July to November the core region weakens (strengthens). Results also suggest an interhemispheric seesaw in the section of the Atlantic Hadley cell, where a stronger upward atmospheric motion south of the equator marks the cold AMO phase. This is consistent with Liu et al. (2020) who suggested that the multidecadal variability in the hemispheric Hadley circulation strength is a response to the AMO, where the intensification in one hemisphere occurs synchronously with the weakening in the other. Nevertheless, uncertainties still exist about the mechanisms by which the AMO influences regional precipitation over South America, mostly because instrumental data contain, in the best case, two full cycles of the AMO (~130 years).

Several attempts have been made to extend instrumental data using terrestrial and marine proxies that indirectly record the past behavior of the AMO (Gray et al., 2004; Mann et al., 2009; Wang et al., 2017; Lapointe et al., 2020). An increasing number of records, summarized by Zhang et al. (2019), indicate that the AMO variability extends several millennia back in time. Recently, Lapointe et al. (2020) provided a reconstruction of the AMO with unprecedented annual resolution. According to this reconstruction, the Little Ice Age (LIA, ~1450–1850 CE; Intergovernmental Panel on Climate Change (IPCC), 2013. Recent evidence also suggests that the AMO played a key role in transition between the Medieval Climate Anomaly (MCA, ~950–1250 CE; IPCC, 2013) and LIA. During the MCA, in the early 1400s, warm Atlantic water intrusion into the Nordic Seas provoked destabilization of subpolar North Atlantic and weakening of the poleward oceanic heat transport followed by intensive cooling of North Atlantic (Arellano-Nava et al., 2022; Lapointe and Bradley, 2021).

Multiple paleoclimate records of the stable oxygen isotope composition ($\delta^{18}O$) from South America (Knudsen et al., 2011; Chiessi et al., 2009; Apaéstegui et al., 2014; Bernal et al., 2016; Flantua et al., 2015; Novello et al., 2018) show typical AMO periodicities (~65 years) and suggest the AMO affected South American hydroclimate in the past. According to records from tropical Andes and south central Brazil, the MCA is characterized as a warm period with a weakened South American monsoon system (Novello et al., 2018; Lüning et al., 2019). Isotopic records also suggest enhanced monsoon during the LIA (Campos et al., 2019; Orrison et al., 2022). On the other hand, speleothems (Novello et al., 2012; Novello et al., 2018) from northeastern Brazil indicate no changes in precipitation amounts during the MCA, but drier LIA period. Utida et al. (2019), however, suggest humid conditions along the coastal area of northeastern Brazil during LIA. At the same time, records from eastern Amazon region indicate variations in the overall aridity over past millennium, with pronounced humid phase in early and to drier conditions in late MCA and LIA (Azevedo et al., 2019). Although the number of available paleo precipitation records from South America significantly increased during the last decade, the relevance of the AMO in the precipitation anomalies over South America during LIA and MCA remains unclear. Therefore, the investigation of how the AMO affects precipitation and how that reflected on isotopic ratios requires the use of isotope-enabled climate models.

In this context, the main objective of this study was to simulate and evaluate the influence of the AMO on atmospheric dynamics, precipitation, and consequently $\delta^{18}O$ of precipitation over South America. For this purpose, the water isotope-enabled version of the Community Earth System Model version 1.2 (iCESM1.2) has been forced with cold and warm AMO-phase SSTs fields. In the following pages, it will also be discussed whether the AMO and related seasonally-dependent responses may potentially have been major drivers of LIA signal found in paleoclimate records (Utida et al., 2019; Campos et al., 2019; Orrison et al., 2022). In addition, $\delta^{18}O$ simulations were compared with a compilation of $\delta^{18}O_p$ published reconstructions within South America.

2. Material and methods

This research is focused on South America, where the main driver of the difference in precipitation between winter dry and summer wet season is South America Monsoon System (SAMS) (Vera et al., 2006; Garreaud et al., 2009). Two main precipitation features of SAMS are the ITCZ, an equatorial cloud band resulting from the low-level convergence of mass and moisture, and the SACZ, a northwest–southeast-oriented cloud band that connects the southern Amazon region with the western portion of the subtropical South Atlantic (Horel et al., 1989; Marengo et al., 2010).

2.1. iCESM model setup

Experiments for this study were carried with a water isotope-enabled version of the Community Earth System Model version 1.2 (iCESM1.2). The iCESM1.2 has active atmosphere, land, ocean, river transport, and sea ice component models linked through a coupler, and also simulates global variations in water isotopic ratios in the atmosphere, land, ocean, and sea ice. The ability of this model to simulate present and past δ18Op patterns has been documented previously (Otto-Bliesner et al., 2016; Zhu et al., 2017; He et al., 2021). Here we assess the influence of the AMO on δ18O of precipitation (™18Op) by analyzing simulations from isotope-enabled version of the Community Earth System Model version 1.2 (iCESM1.2) (Brady et al., 2019). Isotope-enabled models integrate the mass-dependent kinetic fractionation with atmospheric circulation and oceanic evaporation, evaporation and transpiration from land, and the deposition of vapor onto ice. The atmospheric component of iCESM1.2, the isotope-enabled Community Atmosphere Model version 5 (iCAM5.3) (Nusbaumer et al., 2017), is based on the original, non-isotope enabled CAM5 (Neale et al., 2013) and coupled with the interactive Community Land Model version 4 (CLM4; Oleson et al., 2024). Model used in this study is designed so that isotope-specific processes respond directly to simulated physical processes, rather than tuning to match isotopic observations (Brady et al., 2019). Instead of using a fully coupled climate model, in this study the model is forced with prescribed SSTs and configured to use a computational grid of 1.9° latitude × 2.5° longitude and 30 vertical levels from the surface to ~3.5 hPa. Description of the performed experiments can be found in Table 1.

The control experiment (CONTROL) is with prescribed monthly-varying sea-surface temperatures and sea-ice concentrations (SST/SIC) from the Hadley Centre Global Sea Ice and Sea Surface Temperature (HadISST) dataset (Rayner, 2003), while the values for greenhouse gasses, aerosols, ozone, and solar irradiance were fixed at the year 1850 (pre-industrial level). The CONTROL simulation was integrated for 30

Table 1
Description of the experiments performed with the water isotope-enabled version of the Community Earth System Model version 1 (iCESM1.2).

Experiment	Initialization	Sea-surface temperatures (SST) and sea-ice concentrations (SIC)	Simulation
CONTROL	Pre-industrial conditions	HadISST dataset	One ensemble member / 30 yr
CAMO	Pre-industrial conditions	Cold SST anomaly superimposed on the HadISST dataset	Three ensemble members / 50 yr
WAMO	Pre-industrial conditions	Warm SST anomaly superimposed on the HadISST dataset	Three ensemble members/50 yr

years and the first 10 years were discarded as model spin-up. In further two experiments the annual cycle of the SST anomalies, representative of the cold (warm) SST anomaly, is superimposed on the prescribed climatology SST/SIC used in the control run.

The idealized cold and warm SST patterns were computed over time periods with opposite AMO index following Trenberth and Shea (2006) methodology. Both experiments are run as an ensemble of three 50-year long simulations generated with the same model but different initial conditions produced by slight variations in initial atmospheric conditions (Table 1). In order to be on the safe side of soil spin-up, for experiments the spin-up period was extended to 20 years (Yang et al., 1995). The AMO index of Trenberth and Shea (2006) was adopted because it isolates the Atlantic variability from global warming and tropical influences.

The superimposed SST anomalies come from a composite analysis of the HadSST2 dataset (Rayner et al., 2006), after linear detrending to remove the long-term influence. The cold AMO phase comprises the period between 1850 and 1928 and between 1964 and 1995, while the warm AMO phase includes the period between 1929 and 1965 and between 1996 and 2012. Thus, the two experiments, cold AMO (CAMO) and warm AMO (WAMO), only differ by the prescribed SST.

2.2. Main variables and methods used in the analyses

The effects of AMO-related SST over South American climate were evaluated through the differences between CAMO and WAMO experiments, for both precipitation and $\delta^{18}O_p$. The analyses have been applied to the ensemble average. Here we investigated the austral summer (December, January and February, DJF) and autumn season (March, April and May, MAM). We also analyze summer and autumn seasons jointly (December, January, February, March, April, and May, DJFMAM) facilitating simultaneous observation of two major precipitation features, the ITCZ and the South Atlantic Convergence Zone (SACZ) that forms during the mature phase of South American Monsoon System (SAMS) (Garreaud et al., 2009; Sörensson and Menéndez, 2011).

To understand the dynamical mechanisms that caused the changes in precipitation and $\delta^{18}O_p$ we analyzed the upper- and lower-tropospheric circulation.

As the AMO has a strong impact on global atmospheric circulation, changes in Hadley and Walker circulation by comparing vertical velocity (omega; hPa/s) at different pressure levels in the troposphere (Nguyen et al., 2013) were investigated. Hadley cells consist of the ascending branch (represented by upward motion, hence negative vertical velocity) situated in the tropics and associated with enhanced precipitation. At upper-tropospheric levels air is flowing poleward and finally descends in the subtropics (positive vertical velocity), suppressing precipitation. In this study, a latitude-height section 30°N-30°S of vertical velocity, averaged over 80°W-30°W, is analyzed to represent the regional Hadley circulation. The response of the regional Walker circulation over South America, where the ascending branch is situated over the western Amazon region and descending motion occurs east of 40°W from December to March, was analyzed observing the longitude-height section 80°W-30°W, averaged over 0–15°S.

The simulated $\delta^{18}O_p$ responses in each AMO phase have been analyzed in this section. The $\delta^{18}O_p$ denotes the ratio of H218O to H216O in precipitation (Dansgaard, 1964). The relative abundances of stable isotopologues of water (i.e., $^{16}O/^{18}O$) changes due to fractionation that accompany condensation and evaporation processes. Due to slight differences in chemical and physical properties heavier ^{18}O isotopes enter or remain in the liquid or solid phases, while lighter ^{16}O isotopes enter or remain in the vapor phase. The isotopic composition of precipitation is expressed as the per mil (‰) deviation of the heavy-to-light isotope ratio (R) from the Vienna Standard Mean Ocean Water standard (VSMOW) (Kendall and Caldwell, 1998). The $\delta^{18}O_p$ is calculated following eq. (1):

$$\delta^{18}O_p = \left(\frac{\frac{O^{18}}{O^{16}\ sample}}{\frac{O^{18}}{O^{16}\ Standard}} - 1 \right) * 1000‰, \quad (1)$$

Thus, simulated proportions of stable isotopologues (i.e., $^{16}O/^{18}O$) in precipitation vary as a result of natural processes of evaporation and condensation, and because of the effects of temperature and altitude. Consequently, precipitation in each location has its own isotopic ‘fingerprint’.

The statistical significance of these differences was assessed using Student’s *t*-tests at a 95 % confidence level to evaluate whether the means of two different groups were distinct, meaning that the change was significant, or not.

2.3. Compilation of proxy data from paleoclimate archives

According to Lapointe et al. (2020) the coldest AMO anomalies occurred during the LIA (Supplementary material, Fig. S.2). The LIA is also the longest period with a persistent cold anomaly in the North Atlantic over the past ~3 millennia. To test whether the AMO potentially may have been a major driver of the LIA signal found in paleoclimate records, here are compared signals found in paleoclimate records with the simulated spatial footprint during the AMO cold and warm phase, respectively. We defined signals in the LIA and the MCA following the original interpretations of the authors in three categories: “drier” (meaning that the LIA was drier than the MCA), “wetter” (meaning that the LIA was wetter than the MCA) and “neutral” (meaning that the record shows no clear trend in humidity between the LIA and the MCA). We compiled 29 published records of hydroclimate and environmental reconstructions that cover both LIA and MCA (Supplementary material, Table 1).

3. Results

3.1. Changes in precipitation and $\delta^{18}O_p$

The precipitation has a strong seasonal variability over South America and in order to assess the impact of the AMO on two dominant precipitation features, the ITCZ and the SACZ, and consequently $\delta^{18}O_p$, we analyzed simulated austral summer (DJF), austral autumn (MAM), and both seasons together (DJFMAM) (Fig. 1). The DJFMAM season shows continental-scale hydroclimate variability thus enabling capturing the signal of the AMO during the peak of the monsoon season (DJF) as well as the period when ITCZ is reaching its southernmost position (MAM).

During austral summer (DJF), precipitation is significantly reduced over the Atlantic Ocean north of the equator, and in the northern portion of South America (10°N-0°, 75°W-60°W) in the CAMO experiment (Fig. 1a). In contrast, precipitation over most of South America is increased in the CAMO experiment and the highest increase during DJF is simulated over the western Amazon (7°N-10°S, 70°-60°W), the

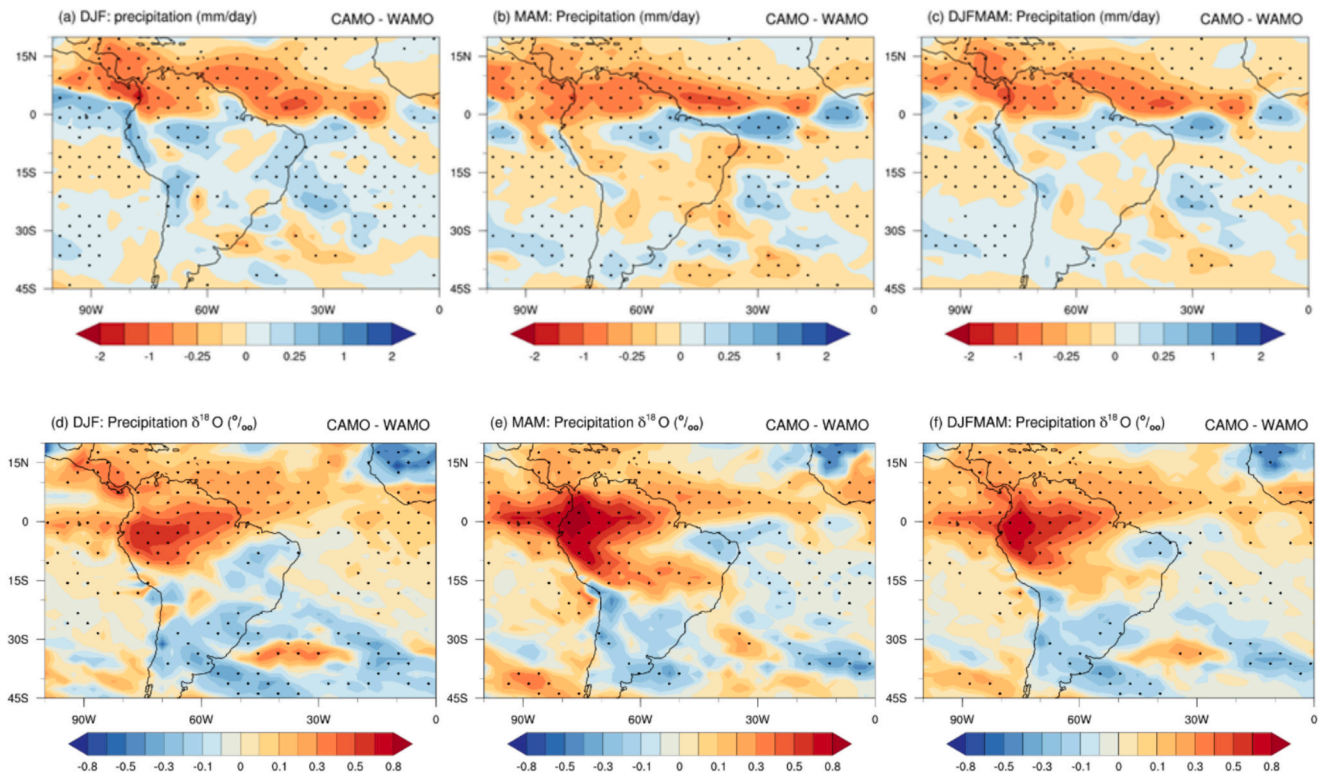

Fig. 1. Precipitation and stable oxygen isotope composition ($\delta^{18}O_p$) (‰) differences between the cold Atlantic Multidecadal Oscillation (CAMO) and the warm Atlantic Multidecadal Oscillation (WAMO) experiments for austral summer (DJF), autumn (MAM) and for December, January, February, March, April, and May (DJFMAM). For precipitation red (blue) shaded areas correspond to drier (wetter) conditions. For in $\delta^{18}O_p$ (‰) red (blue) shaded areas correspond to an increase (decrease). Anomalies that are statistically significant at the 95 % confidence level based on a Student's *t*-test are marked with stippling. Panels a and b modified from Maksic et al. (2022). (For interpretation of the references to colour in this figure legend, the reader is referred to the web version of this article.)

northeastern Brazil (0°-25°S, 55°W-25°W) and the Andes.

During austral autumn (MAM), wetter conditions remain over the northeastern Amazon and in northern northeastern Brazil, while over most of South America precipitation decreased. The highest decreases are simulated over southeastern South America (25°S-40°S, 65°W-50°W), northeastern Brazil and the Andes.

For dynamical processes involved in South American precipitation changes in response to AMO phases and the dynamics of season- and regional-dependent changes in precipitation see Maksic et al. (2022). The DJFMAM mean shows increased precipitation during the cold AMO phase, mainly over the western Amazon region, northern northeastern Brazil and the Andes, while a significant precipitation reduction is present in the northernmost South America. There are also significant inter-hemispheric differences in the amount of precipitation over the Atlantic Ocean, with the largest increase occurring to the south of the equator close to northeastern Brazil and in the South Atlantic, while the largest reduction is observed to the north of the equator (Fig. 1c).

The spatial distribution of $\delta^{18}O_p$ (‰) change between CAMO and WAMO is shown in Fig. 1d-f. During the cold AMO phase, $\delta^{18}O_p$ pattern shows an enriched (positive) signal over the Atlantic Ocean north of the equator and over the entire Amazon region, reaching 15°S in DJF and 20°S in MAM. The highest enrichment in CAMO is simulated over the northwestern coast and the western Amazon (0°-10°S, 80°W-65°W) in MAM. The $\delta^{18}O_p$ values are significantly depleted (negative) in CAMO over the equatorial Atlantic Ocean to the south of the equator, northeastern Brazil and southern South America (20°S-30°S, 55°W-35°W) in MAM. The southeastern region (10°S-20°S, 60°W-35°W) is marked by shifting from negative to positive signal from DJF to MAM.

The DJFMAM mean (Fig. 1c) shows that values remain significantly negative over northeastern Brazil and southern South America (2°S-30°S, 55°W-35°W) and positive over Amazon region and northernmost South America.

3.2. Changes in large-scale circulation

To understand the dynamical mechanisms that caused the changes in precipitation and $\delta^{18}O_p$, we analyzed the extended austral summer (DJFMAM) upper- and lower-tropospheric circulation (Fig. 2 and Fig. 3).

The position of the upper-level anticyclonic circulation, known as the Bolivian High, is the same for both CAMO and WAMO experiments, but the wind circulation is slightly intensified in WAMO (Fig. 2a, b) in comparison with CAMO (Fig. 2a, c). On the other hand, the westerlies (200 hPa) over the North Atlantic Ocean, between the equator and 20°N, are enhanced in CAMO. This inter-hemispheric contrast is reflected in the gradient of precipitation between northern South America and the Amazon region (Fig. 1c). Differences between CAMO and WAMO (Fig. 2c) show that the subtropical jet stream is intensified in the WAMO experiment, in relation to the CAMO experiment, which is related to the intensified Bolivian High. This subtropical jet stream intensification is the highest over the South Atlantic Ocean.

Comparing the 850 hPa wind field anomalies between both AMO phases (Fig. 3), an increased easterly flow reaching 5°S is noted for CAMO. For DJFMAM the Caribbean low-level jet is weakened.

To understand how the ITCZ convection may have affected precipitation and $\delta^{18}O$ we also analyzed the the upper-level divergence (Fig. 4). Differences between 200 hPa divergence fields between AMO phases show an increase in divergence (blue areas) in the same regions where there is an increase in precipitation.

3.3. Changes in atmospheric circulation cells

Fig. 5 reveals the difference (CAMO-WAMO) of the vertical profiles

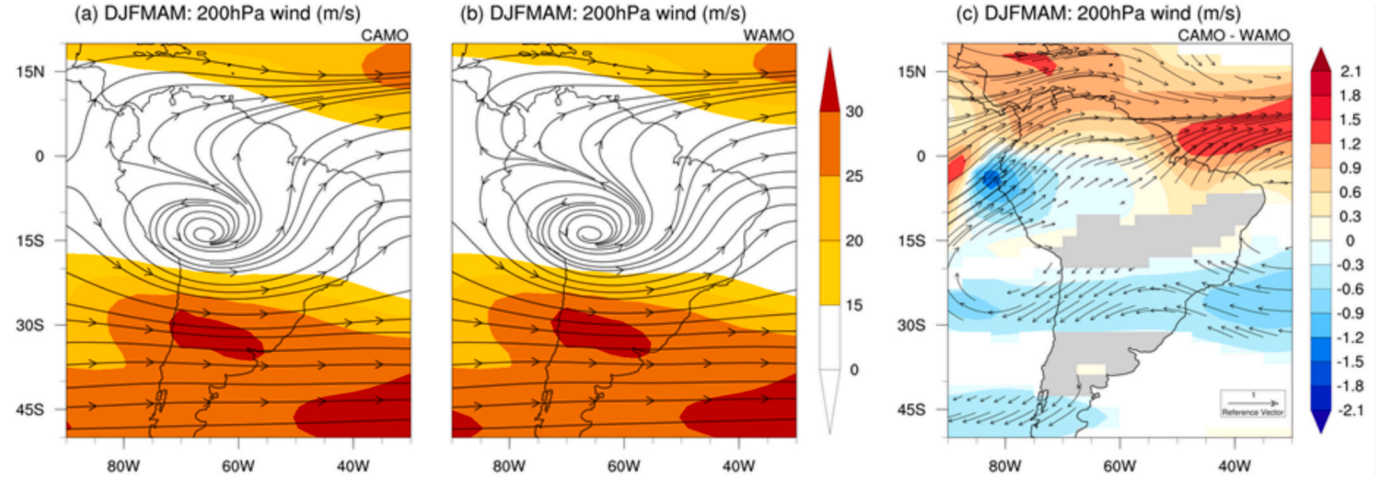

Fig. 2. - The cold Atlantic Multidecadal Oscillation (CAMO) and the warm Atlantic Multidecadal Oscillation (WAMO) seasonal wind vectors and intensity at 200 hPa (m/s) (a,b) and their differences (c) during the extended summer season (December–May; DJFMAM). Only statistically significant differences calculated based on a Student's *t*-test with confidence level of 95 % are shown.

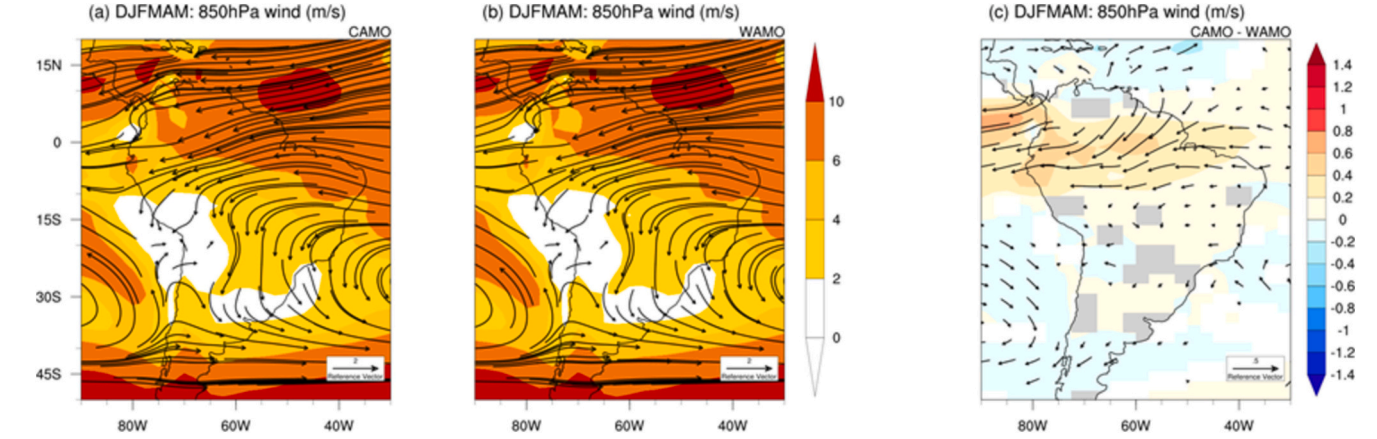

Fig. 3. - Wind vectors and intensity at 850 hPa (m/s) for (a) the cold Multidecadal Oscillation (CAMO) and (b) the warm Atlantic Multidecadal Oscillation (WAMO), as well as for the differences between both phases (CAMO-WAMO) (c) for December–May (DJFMAM). Only statistically significant differences calculated by a Student's *t*-test with confidence level of 95 % are shown.

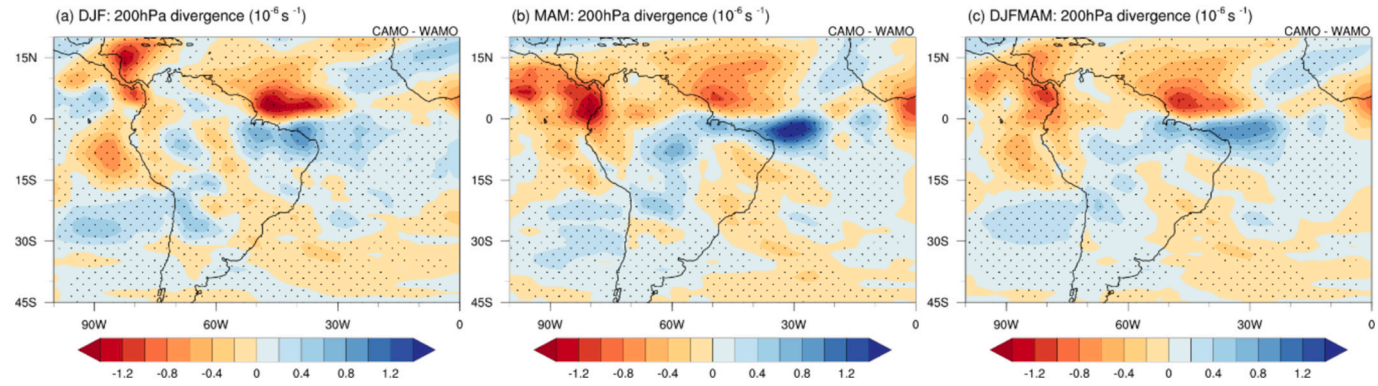

Fig. 4. - Differences in divergence at 200 hPa between for the cold Atlantic Multidecadal Oscillation (CAMO) and the warm Atlantic Multidecadal Oscillation (WAMO) phases, for austral summer (DJF), autumn (MAM) and for December, January, February, March, April, and May (DJFMAM). Stippling areas represent statistically significant (Student's *t*-test at 95 %) differences.

that represent the Hadley and Walker cells.

The Atlantic Hadley cell favors convective activity over the region situated between the 5°N and 15°S. The difference (CAMO-WAMO) of the vertical profile (Fig. 5a) shows high positive anomalies centered between the equator and 15°N, indicating a stronger inter-hemispheric atmospheric circulation. The difference also shows a dipole of negative/positive values south/north of the equator in DJFMAM.

Fig. 5b shows differences in the vertical profile of the Walker

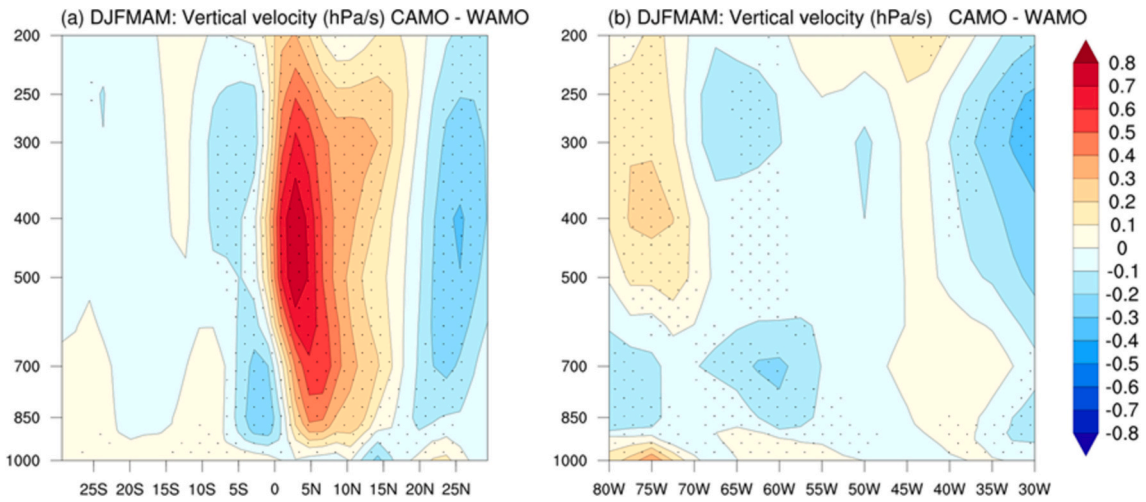

Fig. 5. - Difference between the cold Multidecadal Oscillation (CAMO) and the warm Atlantic Multidecadal Oscillation (WAMO) of vertical pressure velocity (omega; hPa/s) for December–May (DJFMAM). (a) Latitude-height section 30°N - 30°S, averaged over 80°W-30°W, representing the regional Hadley circulation. (b) Longitude-height section 80°W-30°W, averaged over 0–15°S, representing the regional Walker circulation. Anomalies statistically significant at the 95 % confidence level by Student's *t*-test are marked with dots.

circulation. Anomalies show that during the cold AMO phase the ascent of warm and moist air is intensified, contributing to deep convective cloud formation. We also observe positive anomalies in the upper-troposphere east and west of intensification (negative anomaly) field, suggesting potential change in the ascending branch position.

3.4. Paleoclimate reconstructions

Finally, we compare the LIA-MCA $\delta^{18}O$ anomalies from speleothems with simulated CAMO-WAMO $\delta^{18}O_p$ anomalies. We are comparing signals from LIA and MCA, based on the relative difference between LIA and MCA periods, following the original interpretations of the authors. Although we combine as many different paleo records in the compilation as possible (Table S.1), Fig. 6 only shows the approximate location of speleothem records (presented by circles), that provide high-resolution and precisely dated $\delta^{18}O$ time series from the ITCZ and and monsoon regions in South America.

Simulated $\delta^{18}O_p$ anomalies over northeastern Brazil are in agreement with speleothem records from Rio Grande do Norte cave sites (Utida et al., 2022, in revision), as well as with lake sediments from Boqueirão Lake (Utida et al., 2019) located at about 5°S. Significant $\delta^{18}O_p$ enrichment is simulated for the cold AMO over northern South America, equatorial and western Amazon region and the Andes. However, records from the southwestern Amazon region (Della Libera et al., 2022) suggest wetter conditions during the LIA and drier conditions during the MCA. This is in agreement with simulated precipitation (Fig. 1) but not with simulated $\delta^{18}O_p$. Likewise, the simulated $\delta^{18}O_p$ signal differs from speleothem records from the Andes that suggest wetter conditions during the LIA (Bird et al., 2011; Kanner et al., 2013; Apaéstegui et al., 2014).

Simulated anomalies are not statistically significant in eastern Brazil, between 10 and 25°S, and this is also the region with a relative neutral signal between LIA and MCA (Novello et al., 2012; Novello et al., 2018; Wortham et al., 2017; Azevedo et al., 2019). On the other hand, statistically significant negative isotopic anomalies are observed in simulated oxygen isotope ratios over the southern part of tropical South America, which suggest an enhancement of the SASM during cold AMO. This result is in agreement with the signal recorded by speleothems from Cristal cave (Vuille et al., 2012) and partly in agreement with Umajalanta–Chiflonkhakha cave system (Apaéstegui et al., 2018) where records suggest change from wet to dry phase during MCA.

4. Discussion

Due to the complexity of the water cycle, $\delta^{18}O_p$ values in precipitation vary temporally and spatially, being influenced by several environmental factors (e.g., surface air temperature, amount of precipitation, orography, atmospheric humidity, distance from the ocean) (Dansgaard, 1964). Over mid- and high latitude regions, fractionation processes and $\delta^{18}O_p$ variations are primarily governed by the temperature, while those at low latitudes are primarily governed by precipitation (Dansgaard, 1964; Rozanski et al., 2013). In tropical regions, most precipitation arises from deep convection, with vertical motions dominating over horizontal transport, and, via Rayleigh distillation, the high condensation and precipitation results in water vapor with depleted (negative) $\delta^{18}O_p$ (Bowen, 2008; Vuille et al., 2003; Vuille et al., 2012; Campos et al., 2019; Orrison et al., 2022). In areas with less strong convergence, the $\delta^{18}O_p$ depends on a complex interplay between the amount effect, the continental effect (Lachniet, 2009), moisture source and trajectory path (Cruz et al., 2005; Sturm et al., 2007), ocean-atmosphere interactions (Bradley et al., 2003; Vuille and Werner, 2005), and moisture recycling (Ampuero et al., 2020). Given that $\delta^{18}O_p$ integrates information from all parts of the water cycle, proxy records of past hydroclimate preserve signal of large-scale climate dynamics related to changes in distant geographic area, such as North Atlantic SST (Winter et al., 2011; Fensterer et al., 2012). Studies over the past two decades have provided important information on how AMO influences both ITCZ and SAMS, but very little was found in the literature on the isotopic fingerprint of AMO over South America. Statistical analyses show the dominant mode of variability characterized by frequencies of ~60–80 years in several speleothem records (Apaéstegui et al., 2014), but the importance of AMO in the precipitation anomalies during LIA and MCA is still unknown. Recent work by Midhun et al. (2021) finds a globally-distributed, large spatial AMO footprint, but the signal is weak, possibly due to the difficulties of coupled models to appropriately simulate decadal to multidecadal variability (Ault et al., 2012; Kravtsov et al., 2018). Fully coupled models also underestimate the magnitude of decadal variability and fail to produce spatial patterns that match the observed signals (Han et al., 2016).

The present study was designed to determine the effect of AMO on $\delta^{18}O_p$. The results show stronger low level easterly flow in CAMO (Fig. 1c; Fig. 3c) that brings more moisture to the mainland and correlates with the increase in precipitation over the western Amazon (7°N-10°S, 70°-60°W) and coastal northeastern Brazil (Fig. 1c). While the

	Reference	Site name	Lat	Lon	Meters above sea level	Proxy
1	Asmerom et al., 2020	Yok Balum (YOKG), Belize	16.20° N	89.06° W	366	δ13C Speleothem
2	Haug et al., 2001	Cariaco, Venezuela	10.71° N	65.17 ° W		Ocean Sediment Titanium Conc.
3	Wang et al., 2017	Paraiso (PAR01,PAR03), Brazil	4.07 °S	55.45°W	60	δ18O / δ13C Speleothem
4	Apaéstegui et al., 2014	Palestina (PAL03,PAL04), Peru	5.92°S	77.35 °W	870	δ18O / δ13C Speleothem
5	Reuter et al., 2009	Cascayunga Cave, Peru	6.05° S	77.13° W	930	δ18O speleothem
6	Utida et al., 2019	RN caves (Trapia, Furna Nova)	5.14°S	37.62°W	70	δ18O speleothem composite
7	Bird et al., 2011	Pumacocha lake, Peru	10.70 °S	76.06 °W	4300	δ18Olw
8	Kanner et al., 2011	Huagapo cave, Peru	11.27°S	75.79°W	3550	δ18O speleothem
9	Della Libera et al., 2022	Cuíca cave (PIM4 and PIM5), Brazil	11.40°S	60.38°W	310	d18O and d13C speleothems
10	Azevedo et al., 2019	Mata Virgem Cave (MV3), Brazil	11.37°S	47.29°W	365	δ18O and δ13C Speleothem
11	Novello et al., 2012	Diva de Maura and Torinha cave, Brazil	12.22°S	41.34° W	480	Speleothem δ18O
12	Novello et al., 2018	São Bernardo and São Mateus caves, Brazil	13.81°S	46.35°W	631	Speleothem δ18O
13	Thompson et al., 1986	Quelccaya, Peru	13.93°S	70.83° W	5670	δ18Oic
14	Novello et al., 2016	Pau d'Alho (ALHO6), Brazil	15.12°S	56.48°W	600	δ18O stalagmite
15	Wortham et al., 2017	Tamboril Cave, Brazil	16.0°S	47.0°W	700	δ18O, δ13C, 87Sr/86Sr speleothem
16	Apaéstegui et al., 2018	Umajalanta, Bolivia	18.12°S	65.77°W	2650	δ18O Speleothem
17	Vuille et al., 2012	Cristal Cave (CR1), Brazil	24.58°S	48.58°W	130	δ18O Speleothem

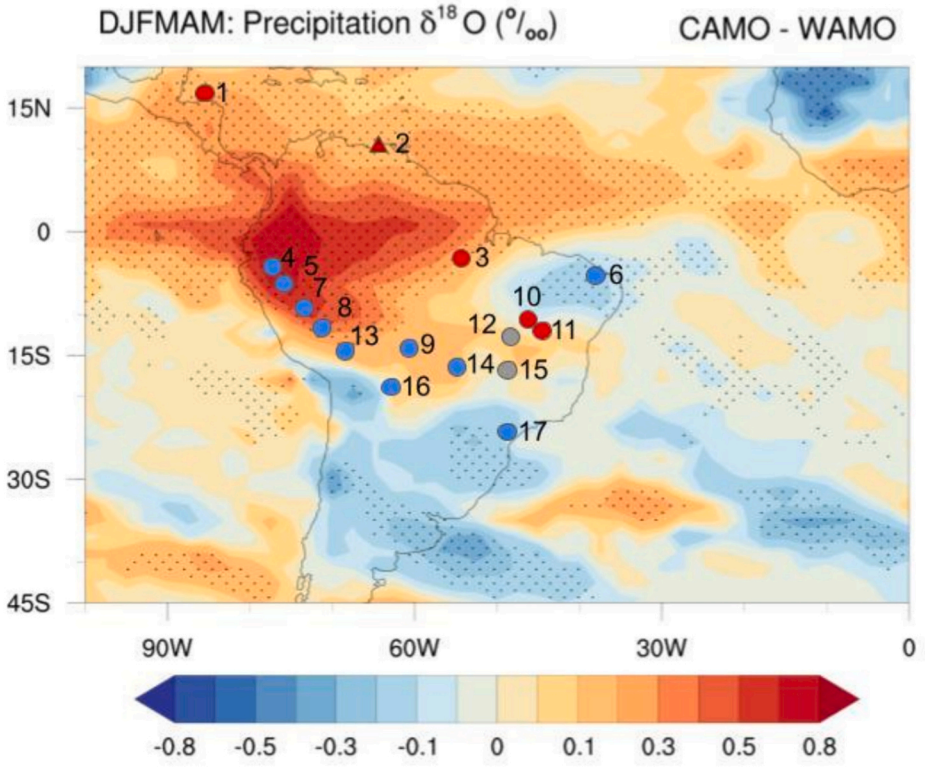

Fig. 6. - Differences between the cold Multidecadal Oscillation (CAMO) and the warm Atlantic Multidecadal Oscillation (WAMO) experiments for $\delta^{18}O_p$. Red (blue) shaded areas correspond to simulated increase (decrease) in $\delta^{18}O_p$ (‰). Anomalies that are statistically significant at the 95 % confidence level based on a Student's t-test are stippled. Paleoclimate record locations: circles, speleothems; triangle, ocean sediment. The anomalies between the Little Ice Age (LIA) and the Medieval Climate Anomaly (MCA), where red (blue) indicate an enriched(depleted) signal in $\delta^{18}O_p$, and gray circles indicate unclear signals (LIA-MCA) in paleoclimate record. For full details about proxies see Supplementary material. (For interpretation of the references to colour in this figure legend, the reader is referred to the web version of this article.)

increase in precipitation during CAMO corresponds with $\delta^{18}O_p$ simulated depletion over northeastern Brazil, significant increase in precipitation in western Amazon during CAMO, which is consistent with observations (Yoon and Zeng, 2009), does not seem to correspond to simulated enriched (positive) $\delta^{18}O_p$ (Fig. 1f). This finding was unexpected and suggests that even when the change in total precipitation amount is significant over the western Amazon this may not be reflected in $\delta^{18}O_p$ depletion. Given that the total precipitation amount changed substantially, the simulation results indicate that different physical processes are compensating for $\delta^{18}O_p$ depletion. This inconsistency may be due to changes in large-scale circulation (Fig. 3c) where the $\delta^{18}O_p$ enrichment signal, related to precipitation reduction throughout the Atlantic Ocean north of the equator, propagates further inland reaching 20°S and diminishes the amount effect. This finding was also reported by Bowen (2008) who observed that isotope seasonality over relatively large regions may be strongly controlled by the strength of convergence over ITCZ. Another potential reason for enriched $\delta^{18}O_p$ values could be a reduction in overall evaporation in CAMO observed over the Amazon region and region under the SAMS influence (Fig. S.3).

In comparison with reconstructions (Fig. 6) we conclude that, contrary to expectations, the simulated $\delta^{18}O_p$ signal differ from speleothem records from the Andes that show wetter conditions during the LIA and $\delta^{18}O_p$ depletion (Bird et al., 2011; Kanner et al., 2013; Apaéstegui et al., 2014). More future analyses are needed to pinpoint the cause of this discrepancy and understand why significant total precipitation amounts change over the western Amazon and Andes are not reflected in $\delta^{18}O_p$

depletion. The reasons for these discrepancies between the reconstructions on the one side and the model on the other side could lie in model systematic biases, limited interaction and feedback in experiments and additional uncontrolled factors. The AMO however may not be the only and primary control of precipitation within South America during LM, and that in different regions other factors were more dominant. It is also important to bear in mind that the possible bias in these responses is in part due to the limited number of ensemble members to provide robust assessments of the forced response.

On the other hand, simulated $\delta^{18}O_p$ agree with speleothems under the SAMS influence (Fig. 1a, d), which show strengthening or southward displacement of the SACZ that occurred during the LIA (Campos et al., 2019; Orrison et al., 2022).

Depletion of $\delta^{18}O_p$ over northeastern Brazil is simulated in both DJF and MAM seasons, although simulated precipitation anomaly is positive in MAM only in its northernmost regions and over the adjacent tropical South Atlantic (Fig. 1a,b). The precipitation increase over the equatorial Atlantic Ocean and northeastern Brazil can be dynamically understood as being associated with changes in the Atlantic ITCZ and the intensified easterly flow. The scientific literature has linked AMO phases and energetically driven meridional shift of ITCZ with precipitation changes over South America (Knight et al., 2006; Ting et al., 2011; Levine et al., 2018). The same mechanism has been associated with drought conditions signal in the Cariaco Basin, located close to the northern limit of the ITCZ, and widespread aridity in the most northern regions of South America and during the LIA (Haug, 2001; Peterson and Haug, 2006). Indeed, the LIA was the longest period with persistent cold anomalies in the North Atlantic (Lapointe et al., 2020). This could support the hypothesis of the ITCZ shifting southwards during the LIA (Haug et al., 2001; Bird et al., 2011; Zhang et al., 2019). Displaced ITCZ could explain dry (wet) signals recorded in the Cariaco Basin and simultaneously wet (dry) signals over northeastern Brazil during LIA (Utida et al., 2019; Utida et al., 2023). However, paleoclimate records from Central America have recently challenged the hypothesis (Polissar et al., 2006; Obrist--Farner et al., 2023; Medina et al., 2023; Asmerom et al., 2020), showing significant spatial variability in hydroclimate during the LIA (Steinman et al., 2022).

Surprisingly, the results of this study do not show substantial differences in the mean position of the Hadley cells and the ITCZ, but changes in intensity. The AMO in experiments presented here has a nearly symmetric effect in modulating the Atlantic ITCZ-related precipitation. Interesting finding is that the equator-symmetric changes present in the simulated precipitation fields are in remarkable agreement with the changes shown in Knight et al. (2006). The results discussed in our previous work (Maksic et al., 2022) suggest an interhemispheric seesaw in Hadley circulation strength and that the section of the Atlantic Hadley cell is marked by a stronger upward air component south of the equator during the cold AMO phase. We also find that the precipitation anomalies over (sub)tropical South America during AMO phases are mainly related to changes in the Atlantic Intertropical Convergence Zone (ITCZ) core strength, where in the cold (warm) AMO phase the core region strengthens (weakens) from February to July, while from July to November the core region weakens (strengthens). Therefore, we interpret the simulated changes in precipitation between different AMO phases as changes in the Atlantic ITCZ core strength. This differs from the findings presented in Steinman et al. (2022) which shows multi century-long southerly shift in the ITCZ accompanied by a decrease in ITCZ strength during the LIA. Thus, although we do not see marked changes in the ITCZ position, it is important to bear in mind the importance of acknowledging the dynamics of season- and regional-dependent ITCZ responses as they are sufficient to produce observed AMO related signals even in the absence of marked changes in the ITCZ position.

Comparison of model-derived signals for regions under the Atlantic ITCZ influence is also consistent with proxy reconstructions (Azevedo et al., 2019; Della Libera et al., 2022; Utida et al., 2023) (Fig. 6). Dipole pattern of both precipitation and $\delta^{18}O_p$ simulated for coastal northeastern Brazil between northern portion and southern portion of northeastern Brazil resembles one found in records (Novello et al., 2012; Novello et al., 2018; Azevedo et al., 2021; Utida et al., 2022, submitted). The results of this study are also in line with studies that suggested the ITCZ expansion/contraction as potential modulator of tropical precipitation changes (Yan et al., 2015; Wodzicki and Rapp, 2016; Denniston et al., 2016; Chiessi et al., 2021). They also complement study that suggests external forcings as main drivers of the Atlantic ITCZ shifts during the last millennium (Roldán-Gómez et al., 2022). This implies that AMO-induced ITCZ seasonal strength changes and ITCZ shifts driven by strong volcanic eruptions during the LIA (Stevenson et al., 2019; Tejedor et al., 2021) contribute jointly to changes in precipitation over South America during the last millennium.

Since the study was limited on one model it should be acknowledged that systematic biases could have influenced results. In addition, the AMO may not in fact be the only and primary control of precipitation $\delta^{18}O_p$ within South America over the last millennium, and that interactions among the three oceans can play an important role in initiating interactions and modulating climate over South America (Wang, 2019; He et al., 2021). It is important to keep in mind that the proxy data reflect differences between LIA and MCA, while the experiments optimally represent only the cold and warm phase from 1850 to 2012. Also, this study is limited to ocean–atmosphere interaction and the climate system is the result of many more complicated feedbacks and interactions. Thus, considerably more work will need to be done to determine which part of the signal found in proxies can be explained by the AMO.

Notwithstanding these limitations, this study support evidence from Utida et al. (2019) who found that regional precipitation along the coastal area of South America was not solely governed by north-south displacements of the ITCZ due to changes in NH climate, but also by the contraction and expansion of the tropical rainbelt. In addition, this mechanism potentially explains the zonal dipole between the coastal area of northeastern Brazil and eastern Amazon region during the LIA (Azevedo et al., 2019; Azevedo et al., 2021). An implication of this finding is the possibility that change in the ITCZ core strength, provoked by persistent cold AMO (Lapointe et al., 2020), contributed to dry conditions over northernmost South America and also increased precipitation along the coastal area of northeastern Brazil during LIA.

5. Conclusions

The findings of this study point out that Atlantic ITCZ strength is sensitive to the Atlantic Multidecadal Oscillation. Hence, teleconnection between the North Atlantic SST and ITCZ strength in simulations presented here drive seasonal variability of precipitation isotope ratios over tropics and subtropics. Model-derived AMO signal for regions under the Atlantic ITCZ influence is consistent with proxy reconstructions and ITCZ strength change potentially explain zonal dipole between northern portion and southern portion of northeastern Brazil, as well as northern portion of northeastern Brazil and eastern Amazon region during the LIA. An implication of this finding is the possibility that change in the ITCZ core strength, provoked by persistent cold AMO, contributed to dry conditions over northernmost South America and also increased precipitation along the coastal area of northeastern Brazil during LIA. These results also suggest that records reflecting annual means should be treated with caution as they potentially record signals of seasonal variability and not ITCZ shift.

Hydroclimatic spatiotemporal patterns in other regions of South America, however, remain puzzling and cannot be explained by AMO, as model-derived AMO signal and signal in records are not consistent. Further research will be necessary to explore which part of the signal found in proxies can be explained by the AMO.

Funding

This study was financed in part by the Coordenação de Aperfeiçoamento de Pessoal de Nível Superior - Brasil (CAPES) - Finance Code 001. Maksic also acknowledges the financial support from FAPESP (grant 2018/23522–6). C.M. Chiessi acknowledges the financial support from FAPESP (grants 2018/15123–4 and 2019/24349–9) and CNPq (grant 312458/2020–7).

CRediT authorship contribution statement

Jelena Maksic: Conceptualization, Data curation, Formal analysis, Investigation, Visualization, Writing – original draft, Writing – review & editing. **Marília Harumi Shimizu:** Conceptualization, Data curation, Formal analysis, Methodology, Validation, Visualization, Writing – review & editing. **Gilvan Sampaio:** Funding acquisition, Investigation, Methodology, Supervision. **Cristiano M. Chiessi:** Investigation, Supervision, Validation, Writing – review & editing. **Matthias Prange:** Conceptualization, Methodology, Software, Supervision, Writing – review & editing. **Mathias Vuille:** Investigation, Validation, Writing – review & editing. **Giselle Utida:** Data curation. **Francisco W. Cruz:** Funding acquisition, Supervision. **Murilo Ruv Lemes:** Visualization.

Declaration of competing interest

The authors declare that they have no known competing financial interests or personal relationships that could have appeared to influence the work reported in this paper.

Appendix A. Supplementary data

Supplementary data to this article can be found online at https://doi.org/10.1016/j.palaeo.2024.112629.

Data availability

Data will be made available on request.

References

Ampuero, A., Stríkis, N.M., Apaéstegui, J., Vuille, Mathias, Novello, V.F., Espinoza, Jhan Carlo, Cruz, F.W., Vonhof, H., Mayta, V.C., Teixeira, V., Cordeiro, Renato Campello, Azevedo, V., Sifeddine, Abdelfettah, 2020. The Forest Effects on the Isotopic Composition of Rainfall in the Northwestern Amazon Basin. J. Geophys. Res. Atmos. 125. https://doi.org/10.1029/2019jd031445.

Apaéstegui, J., Cruz, F.W., Sifeddine, A., Vuille, M., Espinoza, J.C., Guyot, J.L., Khodri, M., Strikis, N., Santos, R.V., Cheng, H., Edwards, L., Carvalho, E., Santini, W., 2014. Hydroclimate variability of the northwestern Amazon Basin near the Andean foothills of Peru related to the South American Monsoon System during the last 1600 years. Climate of the Past 10, 1967–1981. https://doi.org/10.5194/cp-10-1967-2014.

Apaéstegui, J., Cruz, F.W., Vuille, M., Fohlmeister, J., Espinoza, J.C., Sifeddine, A., Strikis, N., Guyot, J.L., Ventura, R., Cheng, H., Edwards, R.L., 2018. Precipitation changes over the eastern Bolivian Andes inferred from speleothem (δ18O) records for the last 1400 years. Earth Planet. Sci. Lett. 494, 124–134. https://doi.org/10.1016/j.epsl.2018.04.048.

Arellano-Nava, B., Halloran, P.R., Boulton, C.A., Scourse, J., Butler, P.G., Reynolds, D.J., Lenton, T.M., 2022. Destabilisation of the Subpolar North Atlantic prior to the Little Ice Age. Nat. Commun. 13. https://doi.org/10.1038/s41467-022-32653-x.

Asmerom, Y., Baldini, J.U.L., Prufer, K.M., Polyak, V.J., Ridley, H.E., Aquino, V.V., Baldini, L.M., Breitenbach, S.F.M., Macpherson, C.G., Kennett, D.J., 2020. Intertropical convergence zone variability in the Neotropics during the Common Era. Sci. Adv. 6. https://doi.org/10.1126/sciadv.aax3644.

Ault, T.R., Cole, J.E., St. George, S., 2012. The amplitude of decadal to multidecadal variability in precipitation simulated by state-of-the-art climate models. Geophys. Res. Lett. 39, n/a–n/a. https://doi.org/10.1029/2012gl053424.

Azevedo, V., Stríkis, N.M., Santos, R.A., de Souza, J.G., Ampuero, A., Cruz, F.W., de Oliveira, P., Iriarte, J., Stumpf, C.F., Vuille, M., Mendes, V.R., 2019. Medieval climate Variability in the eastern Amazon-Cerrado regions and its archeological implications. Sci. Rep. 9. https://doi.org/10.1038/s41598-019-56852-7.

Azevedo, V., Strikis, N.M., Novello, V.F., Roland, C.L., Cruz, F.W., Santos, R.V., Vuille, M., Utida, G., De Andrade, F.R.D., Cheng, H., Edwards, R.L., 2021. Paleovegetation seesaw in Brazil since the late Pleistocene: a multiproxy study of two biomes. Earth Planet. Sci. Lett. 563, 116880. https://doi.org/10.1016/j.epsl.2021.116880.

Bernal, J.P., Cruz, F.W., Stríkis, N.M., Wang, X., Deininger, M., Catunda, M.C.A., Ortega-Obregón, C., Cheng, H., Edwards, R.L., Auler, A.S., 2016. High-resolution Holocene south American monsoon history recorded by a speleothem from Botuverá Cave. Brazil, Earth and Planetary Science Letters 450, 186–196. https://doi.org/10.1016/j.epsl.2016.06.008.

Bird, B.W., Abbott, M.B., Vuille, M., Rodbell, D.T., Stansell, N.D., Rosenmeier, M.F., 2011. A 2,300-year-long annually resolved record of the south American summer monsoon from the Peruvian Andes. Proc. Natl. Acad. Sci. 108, 8583–8588. https://doi.org/10.1073/pnas.1003719108.

Bowen, G., 2008. J.: Spatial analysis of the intra-annual variation of precipitation isotope ratios and its climatological corollaries. J. Geophys. Res. Atmos. 113, n/a–n/a. https://doi.org/10.1029/2007jd009295.

Bradley, R.S., Vuille, M., Hardy, D., Thompson, L.G., 2003. Low latitude ice cores record Pacific Sea surface temperatures. Geophys. Res. Lett. 30. https://doi.org/10.1029/2002gl016546.

Brady, E., Stevenson, S., Bailey, D., Liu, Z., Noone, D., Nusbaumer, J., Otto-Bliesner, B.L., Tabor, C., Tomas, R., Wong, T., Zhang, J., Zhu, J., 2019. The Connected Isotopic Water Cycle in the Community Earth System Model Version 1. Journal of Advances in Modeling Earth Systems 11, 2547–2566. https://doi.org/10.1029/2019ms001663.

Campos, J.L.P.S., Cruz, F.W., Ambrizzi, T., Deininger, M., Vuille, M., Novello, V.F., Stríkis, N.M., 2019. Coherent South American Monsoon Variability during the last Millennium Revealed through High-Resolution Proxy Records. Geophys. Res. Lett. 46, 8261–8270. https://doi.org/10.1029/2019gl082513.

Chiessi, C.M., Mulitza, S., Pätzold, J., Wefer, G., Marengo, J.A., 2009. Possible impact of the Atlantic Multidecadal Oscillation on the south American summer monsoon. Geophys. Res. Lett. 36. https://doi.org/10.1029/2009gl039914.

Chiessi, Cristiano Mazur, Mulitza, S., Taniguchi, Nancy Kazumi, Prange, M., Campos, Mariana Magalhães, Häggi, Christoph, Schefuß, Enno, Lima, M., Frederichs, T., Portilho-Ramos, Rodrigo Costa, Sousa, S.G., Crivellari, S., Cruz, F., 2021. Mid- to Late Holocene Contraction of the Intertropical Convergence Zone Over Northeastern South America. Paleoceanography and Paleoclimatology 36. https://doi.org/10.1029/2020pa003936.

Cruz, F., Karmann, I., Viana, O., Burns, S.A., Ferrari, J.A., Vuille, Mathias, Sial, A.N., Moreira, Marcelo Zacharias, 2005. Stable isotope study of cave percolation waters in subtropical Brazil: Implications for paleoclimate inferences from speleothems. Chem. Geol. 220, 245–262. https://doi.org/10.1016/j.chemgeo.2005.04.001.

Dansgaard, W., 1964. Stable isotopes in precipitation. Tellus 16, 436–468. https://doi.org/10.3402/tellusa.v16i4.8993.

Della Libera, M.E., Novello, V.F., Cruz, F.W., Orrison, R., Vuille, M., Maezumi, S.Y., de Souza, J., Cauhy, J., Campos, J.L.P.S., Ampuero, A., Utida, G., Stríkis, N.M., Stumpf, C.F., Azevedo, V., Zhang, H., Edwards, R.L., Cheng, H., 2022. Paleoclimatic and paleoenvironmental changes in Amazonian lowlands over the last three millennia. Quaternary Science Reviews 279, 107383. https://doi.org/10.1016/j.quascirev.2022.107383.

Denniston, R.F., Ummenhofer, C.C., Wanamaker, A.D., Lachniet, M.S., Villarini, G., Asmerom, Y., Polyak, V.J., Passaro, K.J., Cugley, J., Woods, D., Humphreys, W.F., 2016. Expansion and Contraction of the Indo-Pacific Tropical rain Belt over the last three Millennia. Sci. Rep. 6. https://doi.org/10.1038/srep34485.

Enfield, D.B., Mestas-Nuñez, A.M., Trimble, P.J., 2001. The Atlantic multidecadal oscillation and its relation to rainfall and river flows in the continental US. Geophys. Res. Lett. 28 (10), 2077–2080.

Fensterer, C., Scholz, D., Hoffmann, D., Spötl, C., Pajón, J.M., Mangini, A., 2012. Cuban stalagmite suggests relationship between Caribbean precipitation and the Atlantic Multidecadal Oscillation during the past 1.3 ka. The Holocene 22, 1405–1412. https://doi.org/10.1177/0959683612449759.

Flantua, S.G.A., Hooghiemstra, H., Grimm, E.C., Behling, H., Bush, M.B., González-Arango, C., Gosling, W.D., Ledru, M.-P., Lozano-García, S., Maldonado, A., Prieto, A. R., Rull, V., Van Boxel, J.H., 2015. Updated site compilation of the Latin American Pollen Database. Rev. Palaeobot. Palynol. 223, 104–115. https://doi.org/10.1016/j.revpalbo.2015.09.008.

Folland, C.K., Kates, F.E., 1984. Changes in Decadally Averaged Sea Surface Temperature over the World 1861–1980. Springer eBooks 721–727. https://doi.org/10.1007/978-94-017-4841-4_18.

Garreaud, R.D., Vuille, M., Compagnucci, R., Marengo, J., 2009. Present-day south American climate. Palaeogeography, Palaeoclimatology, Palaeoecology 281, 180–195. https://doi.org/10.1016/j.palaeo.2007.10.032.

Gray, S.T., Graumlich, L.J., Betancourt, J.L., Pederson, G., 2004. T.: a tree-ring based reconstruction of the Atlantic Multidecadal Oscillation since 1567 a.D. Geophys. Res. Lett. 31, n/a–n/a. https://doi.org/10.1029/2004gl019932.

Guan, B., Nigam, S., 2009. Analysis of Atlantic SST variability factoring interbasin links and the secular trend: clarified structure of the Atlantic multidecadal oscillation. J. Climate 22 (15), 4228–4240.

Han, Z., Luo, F., Li, S., Gao, Y., Furevik, Tore, Svendsen, L., 2016. Simulation by CMIP5 models of the Atlantic multidecadal oscillation and its climate impacts. Adv. Atmos. Sci. 33, 1329–1342. https://doi.org/10.1007/s00376-016-5270-4.

Haug, G.H., 2001. Southward Migration of the Intertropical Convergence Zone through the Holocene. Science 293, 1304–1308. https://doi.org/10.1126/science.1059725.

He, Z., Dai, A., Vuille, M., 2021. The joint impacts of Atlantic and Pacific multidecadal variability on south American precipitation and temperature. J. Climate 34, 1–55. https://doi.org/10.1175/jcli-d-21-0081.1.

Horel, J.D., Hahmann, A.N., Geisler, J.E., 1989. An investigation of the Annual Cycle of Convective activity over the Tropical Americas. J. Climate 2, 1388–1403. https://doi.org/10.1175/1520-0442(1989)002%3C1388:AIOTAC%3E2.0.CO;2.

Jones, C., Carvalho, L.M.V., 2018. The influence of the Atlantic multidecadal oscillation on the eastern Andes low-level jet and precipitation in South America. Climate and Atmospheric Science 1. https://doi.org/10.1038/s41612-018-0050-8.
Kanner, L.C., Burns, S.J., Cheng, H., Edwards, R.L., Vuille, M., 2013. High-resolution variability of the south American summer monsoon over the last seven millennia: insights from a speleothem record from the central Peruvian Andes. Quat. Sci. Rev. 75, 1–10. https://doi.org/10.1016/j.quascirev.2013.05.008.
Kayano, M.T., Setzer, A.W., 2018. Nearly Synchronous Multidecadal Oscillations of Surface Air Temperature in Punta Arenas and the Atlantic Multidecadal Oscillation Index. J. Climate 31, 7237–7248. https://doi.org/10.1175/jcli-d-17-0793.1.
Kayano, M.T., Capistrano, V.B., Andreoli, R.V., de Souza, R.A.F., 2016. A further analysis of the tropical Atlantic SST modes and their relations to North-Eastern Brazil rainfall during different phases of Atlantic Multidecadal Oscillation. Int. J. Climatol. 36, 4006–4018. https://doi.org/10.1002/joc.4610.
Kendall, C., Caldwell, E.A., 1998. Chapter 2 - Fundamentals of Isotope Geochemistry. ScienceDirect 51–86.
Knight, J.R., 2009. The Atlantic Multidecadal Oscillation inferred from the forced climate response in coupled general circulation models. J. Climate 22 (7), 1610–1625.
Knight, J.R., Folland, C.K., Scaife, A.A., 2006. Climate impacts of the Atlantic Multidecadal Oscillation. Geophys. Res. Lett. 33. https://doi.org/10.1029/2006gl026242.
Knudsen, M.F., Seidenkrantz, M.-S., Jacobsen, B.H., Kuijpers, A., 2011. Tracking the Atlantic Multidecadal Oscillation through the last 8,000 years. Nat. Commun. 2, 1–8. https://doi.org/10.1038/ncomms1186.
Kravtsov, S., Grimm, C., Gu, S., 2018. Global-scale multidecadal variability missing in state-of-the-art climate models. npj climate and Atmospheric Science 1, 1–10. https://doi.org/10.1038/s41612-018-0044-6.
Krishnamurthy, L., Krishnamurthy, V., 2015. Teleconnections of Indian monsoon rainfall with AMO and Atlantic tripole. Climate Dynam. 46 (7/8), 2269–2285.
Kushnir, Y., 1994. Interdecadal Variations in North Atlantic Sea Surface Temperature and Associated Atmospheric Conditions. J. Climate 7, 141–157. https://doi.org/10.1175/1520-0442(1994)007%3C0141:ivinas%3E2.0.co;2.
Lachniet, M.S., 2009. Climatic and environmental controls on speleothem oxygen-isotope values. Quaternary Science Reviews 28, 412–432. https://doi.org/10.1016/j.quascirev.2008.10.021.
Lapointe, F., Bradley, R.S., 2021. Little Ice Age abruptly triggered by intrusion of Atlantic waters into the Nordic Seas. Sci. Adv. 7. https://doi.org/10.1126/sciadv.abi8230.
Lapointe, F., Bradley, R.S., Francus, P., Balascio, N.L., Abbott, M.B., Stoner, J.S., St-Onge, G., De Coninck, A., Labarre, T., 2020. Annually resolved Atlantic Sea surface temperature variability over the past 2,900 y. Proc. Natl. Acad. Sci. 117, 27171–27178. https://doi.org/10.1073/pnas.2014166117.
Levine, A.F.Z., Frierson, D.M.W., McPhaden, M.J., 2018. AMO Forcing of Multidecadal Pacific ITCZ Variability. J. Climate 31, 5749–5764. https://doi.org/10.1175/jcli-d-17-0810.1.
Loaiza Cerón, W., Andreoli, R.V., Kayano, M.T., Ferreira de Souza, R.A., Jones, C., Carvalho, L.M.V., 2020. The Influence of the Atlantic Multidecadal Oscillation on the Choco Low-Level Jet and Precipitation in Colombia. Atmosphere 11, 174. https://doi.org/10.3390/atmos11020174.
Lüning, S., Gałka, M., Bamonte, F.P., Rodríguez, F.G., Vahrenholt, F., 2019. The medieval climate Anomaly in South America. Quat. Int. 508, 70–87. https://doi.org/10.1016/j.quaint.2018.10.041.
Maksic, J., Shimizu, M.H., Kayano, M.T., Chiessi, C.M., Prange, M., Sampaio, G., 2022. Influence of the Atlantic Multidecadal Oscillation on South American Atmosphere Dynamics and Precipitation. Atmosphere 13, 1778. https://doi.org/10.3390/atmos13111778.
Mann, M.E., Zhang, Z., Rutherford, S., Bradley, R.S., Hughes, M.K., Shindell, D., Ammann, C., Faluvegi, G., Ni, F., 2009. Global Signatures and Dynamical Origins of the Little Ice Age and medieval climate Anomaly. Science 326, 1256–1260. https://doi.org/10.1126/science.1177303.
Marengo, J.A., Liebmann, B., Grimm, A.M., Misra, V., Silva Dias, P.L., Cavalcanti, I.F.A., Carvalho, L.M.V., Berbery, E.H., Ambrizzi, T., Vera, C.S., Saulo, A.C., Nogues-Paegle, J., Zipser, E., Seth, A., Alves, L.M., 2010. Recent developments on the south American monsoon system. Int. J. Climatol. 32, 1–21. https://doi.org/10.1002/joc.2254.
Medina, M.M., Cruz, F.W., Winter, A., Zhang, H., Ampuero, A., Vuille, Mathias, Mayta, V. C., Campos, M.C., Rámirez, Verónica Marcela, Utida, G., Zúñiga, Andrés Camilo, Cheng, H., 2023. Atlantic ITCZ variability during the Holocene based on high-resolution speleothem isotope records from northern Venezuela. Quat. Sci. Rev. 307, 108056. https://doi.org/10.1016/j.quascirev.2023.108056.
Miao, J., Jiang, D., 2021. Multidecadal variations in the east Asian winter monsoon and their relationship with the Atlantic multidecadal oscillation since 1850. J. Climate 34 (18), 7525–7539.
Midhun, M., Stevenson, S., Cole, J.E., 2021. Oxygen Isotopic Signatures of Major climate Modes and Implications for Detectability in Speleothems. Geophys. Res. Lett. 48. https://doi.org/10.1029/2020gl089515.
Neale, R., Richter, J., Conley, A., Park, S., Lauritzen, P., Gettelman, A., Williamson, D., Rasch, P., Vavrus, S., Taylor, M., Collins, W., Nguyen, H., Evans, A., Lucas, C., Smith, I., Timbal, B., 2013. Description of the NCAR Community Atmosphere Model (CAM 4.0), 2010: the Hadley Circulation in Reanalyses: Climatology, Variability, and Change. J. Climate 26, 3357–3376. https://doi.org/10.1175/jcli-d-12-00224.1.
Novello, V.F., Cruz, F., Karmann, I., Burns, S.A., Stríkis, Nicolás Misailidis, Vuille, Mathias, Cheng, H., Lawrence Edwards, R., Christ, R., Frigo, E., Eline, 2012. Multidecadal climate variability in Brazil's Nordeste during the last 3000 years based on speleothem isotope records. Geophys. Res. Lett. 39. https://doi.org/10.1029/2012gl053936 n/a-n/a.
Novello, V.F., Cruz, F.W., Moquet, J.S., Vuille, M., de Paula, M.S., Nunes, D., Edwards, R. L., Cheng, H., Karmann, I., Utida, G., Stríkis, N.M., Campos, J.L.P.S., 2018. Two Millennia of South Atlantic Convergence Zone Variability Reconstructed from Isotopic Proxies. Geophys. Res. Lett. 45, 5045–5051. https://doi.org/10.1029/2017gl076838.
Nusbaumer, J., Wong, T.E., Bardeen, C., Noone, D., 2017. Evaluating hydrological processes in the Community Atmosphere Model Version 5 (CAM5) using stable isotope ratios of water. Journal of Advances in Modeling Earth Systems 9, 949–977. https://doi.org/10.1002/2016ms000839.
Obrist-Farner, J., Steinman, B.A., Stansell, N.D., Maurer, J., 2023. Incoherency in central American Hydroclimate Proxy Records Spanning the last Millennium. Paleoceanography and Paleoclimatology 38. https://doi.org/10.1029/2022pa004445.
Oleson, K.W., Lawrence, D.M., Gordon, B., Flanner, M.G., Kluzek, E., Peter, J., Levis, S., Swenson, S.C., Thornton, E., Feddema, J., Heald, C.L., 2024. Technical description of version 4.0 of the Community Land Model (CLM) | TES-SFA. https://tes-sfa.ornl.gov/bibcite/reference/131 last access: 17 July 2023.
Orrison, R., Vuille, M., Smerdon, J.E., Apaéstegui, J., Azevedo, V., Campos, J.L.P.S., Cruz, F.W., Della Libera, M.E., Stríkis, N.M., 2022. South American Summer Monsoon variability over the last millennium in paleoclimate records and isotope-enabled climate models. Clim. Past 18, 2045–2062. https://doi.org/10.5194/cp-18-2045-2022.
Otto-Bliesner, B.L., Brady, E.C., Fasullo, J.T., Jahn, A., Landrum, L., Stevenson, S., Rosenbloom, N., Mai, A., Strand, W.G., 2016. Climate Variability and Change since 850 CE: An Ensemble Approach with the Community Earth System Model. Bull. Am. Meteorol. Soc. 97, 735–754. https://doi.org/10.1175/bams-d-14-00233.1.
Peterson, L.C., Haug, G.H., 2006. Variability in the mean latitude of the Atlantic Intertropical Convergence Zone as recorded by riverine input of sediments to the Cariaco Basin (Venezuela). Palaeogeogr. Palaeoclimatol. Palaeoecol. 234, 97–113. https://doi.org/10.1016/j.palaeo.2005.10.021.
Polissar, P.J., Abbott, M.B., Wolfe, A.P., 2006. Maximiliano Bezada, Rull, V., and Bradley, R. S.: Solar modulation of Little Ice Age climate in the tropical Andes. Proc. Natl. Acad. Sci. U. S. A. 103, 8937–8942. https://doi.org/10.1073/pnas.0603118103.
Qin, M., Dai, A., Hua, W., 2020. Quantifying contributions of internal variability and external forcing to Atlantic multidecadal variability since 1870. Geophys. Res. Lett. 47 (22).
Rayner, N.A., 2003. Global analyses of sea surface temperature, sea ice, and night marine air temperature since the late nineteenth century. J. Geophys. Res. 108. https://doi.org/10.1029/2002jd002670.
Rayner, N.A., Brohan, P., Parker, D.E., Folland, C.K., Kennedy, J.J., Vanicek, M., Ansell, T.J., Tett, S.F.B., 2006. Improved analyses of changes and Uncertainties in Sea Surface Temperature measured in Situ since the Mid-Nineteenth Century: the HadSST2 Dataset. J. Climate 19, 446–469. https://doi.org/10.1175/jcli3637.1.
Roldán-Gómez, P.J., González-Rouco, J.F., Melo-Aguilar, C., Smerdon, J.E., 2022. The Role of Internal Variability in ITCZ changes over the last Millennium. Geophys. Res. Lett. 49. https://doi.org/10.1029/2021gl096487.
Rozanski, K., Araguás-Araguás, L., Gonfiantini, R., 2013. Isotopic patterns in Modern Global Precipitation. Climate Change in Continental Isotopic Records 1–36. https://doi.org/10.1029/gm078p0001.
Schlesinger, M.E., Ramankutty, N., 1994. An oscillation in the global climate system of period 65–70 years. Nature 367, 723–726. https://doi.org/10.1038/367723a0.
Seager, R., Naik, N., Baethgen, W., Robertson, A., Kushnir, Y., Nakamura, J., Jurburg, S., 2010. Tropical Oceanic Causes of Interannual to Multidecadal Precipitation Variability in Southeast South America over the Past Century*. J. Climate 23, 5517–5539. https://doi.org/10.1175/2010jcli3578.1.
Sörensson, A., Menéndez, C.G., 2011. Summer soil–precipitation coupling in South America. Tellus A 63, 56–68. https://doi.org/10.1111/j.1600-0870.2010.00468.x.
Steinman, B.A., Stansell, N.D., Mann, M.E., Cooke, C.R., Abbott, M.B., Vuille, Mathias, Bird, B.W., Lachniet, M.S., Fernandez, A., 2022. Interhemispheric antiphasing of neotropical precipitation during the past millennium. Proc. Natl. Acad. Sci. 119. https://doi.org/10.1073/pnas.2120015119.
Stevenson, S., Otto-Bliesner, B.L., Brady, E.C., Nusbaumer, J., Tabor, C., Tomas, R., Noone, D.C., Liu, Z., 2019. Volcanic Eruption Signatures in the Isotope-Enabled last Millennium Ensemble. Paleoceanography and Paleoclimatology 34, 1534–1552. https://doi.org/10.1029/2019pa003625.
Sturm, C., Vimeux, F., Krinner, G., 2007. Intraseasonal variability in South America recorded in stable water isotopes. J. Geophys. Res. 112. https://doi.org/10.1029/2006jd008298.
Sutton, R.T., Hodson, D.L., 2005. Atlantic Ocean forcing of north American and European summer climate. Science 309 (5731), 115–118.
Tejedor, E., Steiger, N.J., Smerdon, J.E., Serrano-Notivoli, R., Vuille, M., 2021. Global hydroclimatic response to tropical volcanic eruptions over the last millennium. Proc. Natl. Acad. Sci. 118, e2019145118. https://doi.org/10.1073/pnas.2019145118.
Ting, M., Kushnir, Y., Seager, R., Li, C., 2009. Forced and internal twentieth-century SST trends in the North Atlantic. J. Climate 22 (6), 1469–1481.
Ting, M., Kushnir, Y., Seager, R., Li, C., 2011. Robust features of Atlantic multi-decadal variability and its climate impacts. Geophys. Res. Lett. 38, n/a–n/a. https://doi.org/10.1029/2011gl048712.
Trenberth, K.E., Shea, D.J., 2006. Atlantic hurricanes and natural variability in 2005. Geophys. Res. Lett. 33. https://doi.org/10.1029/2006gl026894.
Utida, G., Cruz, F.W., Etourneau, J., Bouloubassi, I., Schefuß, E., Vuille, M., Turcq, B., 2019. Tropical South Atlantic influence on Northeastern Brazil precipitation and ITCZ displacement during the past 2300 years. Scientific reports 9 (1), 1698.
Utida, G., Cruz, F.W., Vuille, M., Ampuero, A., Novello, V.F., Maksic, J., Sampaio, G., Cheng, H., Zhang, H., Dias de Andrade, F.R., Edwards, R.L., 2023. Spatiotemporal

ITCZ dynamics during the last three millennia in Northeastern Brazil and related impacts in modern human history. Climate of the Past [preprint] 1–38. https://doi.org/10.5194/cp-2023-2.

Vera, C., Higgins, W., Amador, J., Ambrizzi, T., Garreaud, R., Gochis, D., Gutzler, D., Lettenmaier, D., Marengo, J., Mechoso, C.R., Nogues-Paegle, J., Dias, P.L.S., Zhang, C., 2006. Toward a Unified View of the American Monsoon Systems. J. Climate 19, 4977–5000. https://doi.org/10.1175/JCLI3896.1.

Vuille, M., Werner, M., 2005. Stable isotopes in precipitation recording south American summer monsoon and ENSO variability: observations and model results. Climate Dynam. 25, 401–413. https://doi.org/10.1007/s00382-005-0049-9.

Vuille, M., Bradley, R.S., Werner, M., Healy, R., Keimig, F., 2003. Modeling δ18O in precipitation over the tropical Americas: 1. Interannual variability and climatic controls. J. Geophys. Res. 108. https://doi.org/10.1029/2001jd002038.

Vuille, M., Burns, S.J., Taylor, B.L., Cruz, F.W., Bird, B.W., Abbott, M.B., Kanner, L.C., Cheng, H., Novello, V.F., 2012. A review of the south American monsoon history as recorded in stable isotopic proxies over the past two millennia. Climate of the Past 8, 1309–1321. https://doi.org/10.5194/cp-8-1309-2012.

Wang, C., 2019. Three-ocean interactions and climate variability: a review and perspective. Climate Dynam. 53, 5119–5136. https://doi.org/10.1007/s00382-019-04930-x.

Wang, C., Dong, S., Evan, A.T., Foltz, G.R., Lee, S.K., 2012. Multidecadal covariability of North Atlantic Sea surface temperature, african dust, Sahel rainfall, and Atlantic hurricanes. J. Climate 25 (15), 5404–5415.

Wang, J., Yang, B., Ljungqvist, F.C., Luterbacher, J., Osborn, Timothy J., Briffa, K.R., Zorita, E., 2017. Internal and external forcing of multidecadal Atlantic climate variability over the past 1,200 years. Nat. Geosci. 10, 512–517. https://doi.org/10.1038/ngeo2962.

Winter, A., Miller, T., Kushnir, Y., Sinha, A., Timmermann, A., Jury, M.R., Gallup, C., Cheng, H., Edwards, R.L., 2011. Evidence for 800 years of North Atlantic multi-decadal variability from a Puerto Rican speleothem. Earth Planet. Sci. Lett. 308, 23–28. https://doi.org/10.1016/j.epsl.2011.05.028.

Wodzicki, K.R., Rapp, A.D., 2016. Long-term characterization of the Pacific ITCZ using TRMM, GPCP, and ERA-Interim. Journal of Geophysical Research: Atmospheres 121, 3153–3170. https://doi.org/10.1002/2015jd024458.

Wortham, B.E., Wong, C.I., Lucas, McGee, D., Montañez, I.P., Rasbury, E. Troy, Cooper, K.M., Sharp, W.D., Glessner, Justin J.G., Christ, R., 2017. Assessing response of local moisture conditions in Central Brazil to variability in regional monsoon intensity using speleothem 87Sr/86Sr values. Earth Planet. Sci. Lett. 463, 310–322. https://doi.org/10.1016/j.epsl.2017.01.034.

Yan, H., Wei, W., Soon, W., An, Z., Zhou, W., Liu, Z., Wang, Y., Carter, R.M., 2015. Dynamics of the intertropical convergence zone over the western Pacific during the Little Ice Age. Nat. Geosci. 8, 315–320. https://doi.org/10.1038/ngeo2375.

Yan, X., Zhang, R., Knutson, T.R., 2019. A multivariate AMV index and associated discrepancies between observed and CMIP5 externally forced AMV. Geophys. Res. Lett. 46 (8), 4421–4431.

Yang, Z.-L., Dickinson, R.E., Henderson-Sellers, A., Pitman, A.J., 1995. Preliminary study of spin-up processes in land surface models with the first stage data of Project for Intercomparison of Land Surface Parameterization Schemes phase 1(a). J. Geophys. Res. 100, 16553. https://doi.org/10.1029/95jd01076.

Yoon, J.-H., Zeng, N., 2009. An Atlantic influence on Amazon rainfall. Climate Dynam. 34, 249–264. https://doi.org/10.1007/s00382-009-0551-6.

Zhang, R., Delworth, T.L., 2006. Impact of Atlantic multidecadal oscillations on India/Sahel rainfall and Atlantic hurricanes. Geophys. Res. Lett. 33 (17).

Zhang, R., Sutton, R., Danabasoglu, G., Kwon, Y., Marsh, R., Yeager, S.G., Amrhein, D.E., Little, C.M., 2019. A Review of the Role of the Atlantic Meridional Overturning Circulation in Atlantic Multidecadal Variability and Associated climate Impacts. Rev. Geophys. 57, 316–375. https://doi.org/10.1029/2019rg000644.

Zhu, J., Liu, Z., Brady, E., Otto-Bliesner, B., Zhang, J., Noone, D., Tomas, R., Nusbaumer, J., Wong, T., Jahn, A., Tabor, C., 2017. Reduced ENSO variability at the LGM revealed by an isotope-enabled Earth system model. Geophys. Res. Lett. 44, 6984–6992. https://doi.org/10.1002/2017gl073406.